

# Effect of physical aging on nano- and macroscopic properties of poly(methyl methacrylate) glass

A. Wypych<sup>a,b,c</sup>, E. Duval<sup>b</sup>, G. Boiteux<sup>c</sup>, J. Ulanski<sup>a,\*</sup>, L. David<sup>c</sup>, A. Mermet<sup>b</sup>

<sup>a</sup> Department of Molecular Physics, Technical University of Lodz, ul. Zeromskiego 116, 90-924 Lodz, Poland

<sup>b</sup> Laboratoire de Physico-Chimie des Matériaux Luminescents, UMR CNRS 5620, Université Claude Bernard Lyon 1, 43, Bd. du 11 Novembre, 69622 Villeurbanne Cedex, France

<sup>c</sup> Laboratoire des Matériaux Polymères et Biomatériaux, UMR CNRS 5627/IMP, Université Claude Bernard Lyon1, 43, Bd. du 11 Novembre, 69622 Villeurbanne Cedex, France

Received 22 June 2005; received in revised form 4 October 2005; accepted 25 October 2005

Available online 14 November 2005

## Abstract

Physical aging of amorphous poly(methyl methacrylate) has been studied by low frequency Raman scattering, broad-band dielectric spectroscopy, low frequency high resolution mechanical spectroscopy and differential scanning calorimetry. The material was subjected to different thermal histories by isothermal aging. A consistent relationship between the changes caused by the physical aging in nanostructure and molecular dynamics has been found. The aging makes the structure more homogeneous at a scale of few nanometers, bringing it to a structural state of lower energy. These structural changes affect mainly the  $\alpha$ -relaxation, however, some increase in the relaxation strength as well as an increase in the activation energy of the  $\beta$ -relaxation is also observed.

© 2006 Elsevier Ltd. All rights reserved.

**Keywords:** Poly(methyl methacrylate); Physical aging; Nanostructure

## 1. Introduction

Amorphous polymers below the glass transition temperature ( $T_g$ ) are far from their thermodynamic equilibrium. Indeed, fast cooling from temperature above  $T_g$  to temperature lower than glass transition temperature leads to high viscosity and lower mobility of the system resulting in a non-equilibrium structure. In glasses, in a time scale a molecular (and structural) rearrangements appear, in which the chains tend to reach thermodynamic equilibrium. This process is called ‘physical aging’ and was introduced by Struik [1] to distinguish these effects from other aging processes such as chemical reactions, i.e. degradations. The aging phenomenon affects thermodynamical parameters [1–4], influences molecular dynamics [5–8] and changes the structure at nanometric level [9]. Different thermo-mechanical treatments may induce structural rearrangements in amorphous polymers. The aging temperature and the aging time are regarded as main factors in the case of physical aging phenomenon, but structural changes also may

be induced by plastic deformation [11] or by low molecular weight host molecules like methanol in poly(methyl methacrylate) [9,12]. The investigations carried out so far have been performed by many authors and by using different techniques. Nevertheless, the different aging procedures applied during these experiments and different material parameters like: molecular mass or tacticity, make direct comparison between them difficult. The involvement of molecular relaxations in the physical aging process is clear, but the choice of the relevant structural parameters that determine molecular mobility in polymers is still debated. In the case of poly(methyl methacrylate) (PMMA) the involvement of the sub- $T_g$   $\beta$ -relaxation is especially a contentious matter. An issue connected with this, it is the relation between structural relaxation and the disordered polymer structure at the nanometric level. For these reasons the studies on physical aging phenomena with the use of different experimental techniques for one material aged due to some normalized procedure, are still up to date and purposeful. They allow a deeper understanding of the relation between the structural state and dynamics of glass-forming systems.

In the present work, the aging processes were studied for amorphous PMMA aged for different times and at different temperatures in glassy state. Aging effects were investigated by: Low frequency Raman scattering (LFRS), broadband

\* Corresponding author. Tel.: +48 42 631 32 05; fax: +48 42 631 32 18.  
E-mail address: [julanski@p.lodz.pl](mailto:julanski@p.lodz.pl) (J. Ulanski).

dielectric spectroscopy (BDS), low frequency high resolution mechanical spectroscopy (LFHRMS) and differential scanning calorimetry (DSC).

The LFRS of amorphous polymers arises from the partial localization of acoustic vibrational modes which, being non-propagative in the disordered structures, become Raman active. Hence they give rise to a broad feature at frequencies lower than ca.  $200\text{ cm}^{-1}$ . The so-called Boson peak located between 10 and  $30\text{ cm}^{-1}$  is a characteristic feature of amorphous materials. It appears as an excess of vibrational density of states (VDOS) in comparison to that predicted by the Debye theory. The Boson peak is, therefore, sensitive to the nanostructure changes and gives information about the size of the heterogeneities in glassy matter [9,11,12]. In this work the obtained results are analysed in frame of the model of non-homogenous nanostructure of glasses proposed by Duval et al., in which it is assumed that the more strongly bonded regions (more cohesive nanodomains) are separated by weakly bonded channels (soft zones) [13].

The application of BDS and LFHRMS allows to investigate the influence of the physical aging on dielectric and dynamic-mechanical properties of PMMA. The information received through applying different techniques makes it possible to understand better the correlations between the thermal history, structure at different size scale and relaxation phenomena in glass-forming systems.

## 2. Experimental

### 2.1. Materials

The investigated polymer is a PMMA for optical purposes and has a weight average molecular mass ( $M_w$ ) equal  $120,000\text{ g/mol}$  with polydispersity- $I_p=1.6$  as assessed by size exclusion chromatography (SEC) measurements. The NMR measurements ( $^1\text{H}$  and  $^{13}\text{C}$ ) indicate the presence of syndiotactic triads (rr) of about 0.48, isotactic triads (mm) 0.09 and atactic triads (mr) 0.43. These values are very similar to the theoretical data of fully atactic PMMA.

The glass transition temperature  $T_g=111\text{ }^\circ\text{C}$  was determined from the DSC measurements (mid point) with a heating rate of  $10\text{ K/min}$ .

The LFRS and DSC measurements were performed for the extrusion grade pellets, while the BDS and LFHRMS measurements were performed for the films. Before the aging, all the pellets were heated above  $T_g$  in nitrogen atmosphere (30 min at  $135\text{ }^\circ\text{C}$ ) in order to erase its earlier thermal and mechanical history (reference state). The PMMA films with a thickness of ca.  $0.2\text{ mm}$  were compression-moulded at  $150\text{ }^\circ\text{C}$  during ca. 10 min under the pressure of ca. 4 bars. To eliminate the internal stresses, the films were additionally annealed without pressure at  $150\text{ }^\circ\text{C}$  for about 5–10 min. The samples prepared according to this procedure were quenched to room temperature with a rate of about  $75\text{ K/min}$ . Some of them were investigated immediately after the quenching as the reference (not aged samples). Other samples

were aged by: (a) annealing at  $95$  and  $80\text{ }^\circ\text{C}$  (i.e.  $T_g-16$  and  $T_g-31\text{ }^\circ\text{C}$ , respectively) in nitrogen atmosphere during 3 weeks, or (b) storage at room temperature ( $25\text{ }^\circ\text{C}$ ) for about 9 months. The pellets and the films were aged simultaneously in the same conditions.

To rule out any additional effects (like degradation) from the obtained results, SEC measurements and Raman spectroscopy in conventional frequency range were applied. SEC measurements performed for PMMA samples after different thermal treatments have exhibited only negligible changes of the molecular weight. Raman spectra around  $1640\text{ cm}^{-1}$  (the location of PMMA monomer's band, which is ascribed to  $\text{C}=\text{C}$  vibrations) were also studied to detect possible depolymerization, which might appear during thermal treatments [14] and no such effects were detected.

### 2.2. Techniques

The physical aging affects the macroscopic properties (enthalpy and entropy level) [2,3] of amorphous polymers, but also cause the changes in the polymer structure at nanoscale. To investigate this effect in PMMA the LFRS was used since it enables the investigation of the structure (and its evolution) at nanometric level by observing the Boson peak. The Raman Boson peak reflects principally the low energy VDOS excess, comparing with Debye regime. Thus, it is a source of information on the supermolecular structure of glasses. Such a relation is expressed by Eq. (1), which gives the LFRS intensity  $I(\omega)$  for Stokes scattering:

$$I(\omega) = C(\omega)g(\omega)\frac{n(\omega) + 1}{\omega} \quad (1)$$

where:  $C(\omega)$  is the light-vibration coupling coefficient,  $g(\omega)$  is the VDOS,  $\omega$  is the frequency and  $n(\omega)$  is the Bose factor. The reduced intensity:  $I_R(\omega)=I(\omega)/[n(\omega) + 1]$  is approximately proportional to the VDOS. The Boson peak in such representation appears as a shoulder on a low-frequency wing of bell-shaped curve (acoustic band), which has a maximum at about  $80\text{ cm}^{-1}$ . For easier comparisons the normalized form was chosen, which is given by Eq. (2):

$$I_n(\omega) = \frac{I(\omega)}{[n(\omega) + 1]\omega} \quad (2)$$

In this representation the Boson peak appears as the band located between 10 and  $30\text{ cm}^{-1}$ . In order to compare LFRS intensities of reference and aged samples, they were additionally normalized at the maximum of acoustic band visible in the reduced Raman spectra. This band is believed not to be affected by physical aging since the high cohesive domains are not involved in the reorganization of the structure in nanoscale. As a result, the normalized Raman spectra presented in Fig. 1 are perfectly matched in higher frequencies, while the low frequency region reveals changes caused by physical aging.

The LFRS was analysed with a high-resolution five-grating monochromator equipped with a photon counting system. The sample was illuminated with an argon laser beam of

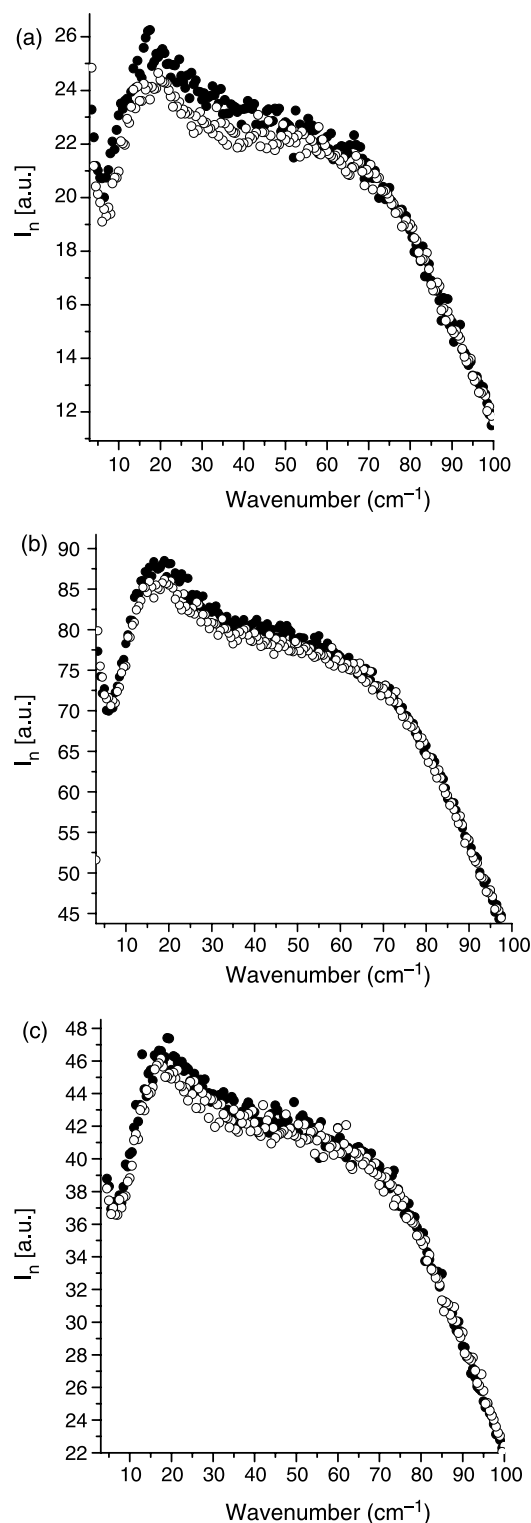


Fig. 1. Comparisons of normalized LFRS spectra: (a) reference sample and sample annealed 3 weeks at 95 °C; (b) reference sample and sample annealed 3 weeks at 80 °C; (c) reference sample and sample aged at 25 °C during 9 months. The full and empty circles correspond to reference and aged samples, respectively.

wavelength 514.5 nm. The Raman spectra were measured at room temperature along the direction perpendicular to the incident light polarization (HV configuration) in a spectral range: 2–200  $\text{cm}^{-1}$ .

BDS measurements were performed in the frequency range of 0.01 Hz–1 MHz and in the temperature range –125 to +130 °C (in steps of 5 K) using a Novocontrol broadband dielectric spectrometer. To provide good contact the circular gold electrodes with 20 mm diameter were evaporated onto the polymer films (sandwich-type configuration). The obtained complex dielectric function ( $\epsilon^*$ ):

$$\epsilon^* = \epsilon' - i\epsilon'' \quad (3)$$

(where:  $\epsilon'$  and  $\epsilon''$  are the real part and the imaginary or loss part, respectively, while  $\omega$  is a circular frequency and  $i = \sqrt{-1}$ ) has been analysed by WinFit program supplied by Novocontrol. The data was fitted using Havriliak–Negami (HN) function according to:

$$\epsilon^* = \epsilon_\infty + \frac{\Delta\epsilon}{(1 + (i\omega\tau)^{\alpha_{\text{HN}}})^{\beta_{\text{HN}}}} \quad (4)$$

where:  $\epsilon_\infty$  is the real permittivity for high frequencies,  $\Delta\epsilon$  is the relaxation strength and is proportional to the height of the maximum peak in  $\epsilon''$ ,  $\tau$  is relaxation time and  $\alpha_{\text{HN}}$  and  $\beta_{\text{HN}}$  are Havriliak–Negami (HN) parameters which correspond, respectively, to the width and asymmetry of relaxation function.

In order to confirm the effect of aging on the  $\beta$  relaxation the dynamic behaviour of PMMA aged 3 weeks at 80 °C (i.e.  $T_g - 31$  °C) was assessed by low-frequency high-resolution mechanical spectroscopy (LFHRMS). The home-made spectrometer described elsewhere [15,16] makes it possible to measure the complex shear modulus  $G^*(j,\omega) = G'(\omega) + jG''(\omega)$  as a function of  $T$  and angular frequency  $\omega$ . The ratio  $G''/G'$  is defined as the loss coefficient  $\text{tg } \phi$ . The complex elastic modulus was measured at constant frequency (at 1 Hz) by temperature scanning from –120 to  $T_g + 25$  °C; next the sample was cooled at 1 °C/min, leading it to the so-called ‘quenched state’. Such a protocol allows us to compare data for those aged and quenched state without any handling of the specimen between the two sets of results. The relative shear strain does not exceed  $10^{-4}$ . This low level ensures that the measurements are performed in the linear regime and any structural evolution was not induced by deformation.

The DSC measurements were made using the DSC 2920-TA instrument. For each sample two temperature scans were performed in the temperature range: 20–140 °C at a heating rate 10 K/min. All samples, with a weight of about 10 mg each, were sealed in aluminium pans and the measurements were performed under a high purity helium atmosphere.

### 3. Results

In Fig. 1(a) the normalized spectrum  $I_n(\omega)$  for the reference PMMA sample (full circles) is compared with the spectra for the PMMA sample after 3 weeks of thermal aging at 95 °C (empty circles). In Fig. 1(b) and (c) similar comparisons are presented for the sample aged during 3 weeks at 80 °C and for the sample after long room temperature aging, respectively. The maximum of the Boson peak appears in a spectrum at ca.

$20 \text{ cm}^{-1}$ . It is seen that the Raman scattering around this region is weaker for the aged samples. The previous measurements and the Lorentzian shape of the quasi-elastic scattering show that the decrease of the Boson peak is due to the decrease of the harmonic VDOS [9,10,14]. It is worth noting that for the samples annealed at temperatures close to  $T_g$  the intensity of the Raman scattering decreases also in the higher frequency part (up to  $60 \text{ cm}^{-1}$ ). The magnitude of the observed changes is dependent on the aging temperature and decreases when the annealing temperature becomes lower. In the case of the sample aged at room temperature for a long time the changes are very weak and only the Boson peak region (up to  $35 \text{ cm}^{-1}$ ) is affected.

Fig. 2 shows 3-dimensional plot for the PMMA reference sample of the frequency-temperature dependences of  $\epsilon''$ . The three dashed lines indicate an evolution in the temperature and frequency of the  $\gamma$ - $\beta$ -and  $\alpha$ -relaxation processes. At frequency of 1 Hz they are located at about:  $-100$ ,  $0$  and  $110$  °C, respectively. The  $\alpha$ -relaxation is associated with the glass transition temperature. The  $\beta$ -relaxation, very well pronounced in PMMA, is connected with rotation or conformational changes of the ester moiety ( $-\text{COOCH}_3$ ) around the bond linked with the main chain, while the  $\gamma$ -relaxation is due to rotation of the  $\alpha$ -methyl group bonded to the main chain or can be connected with small amounts of water absorbed from the environment during the preparation of the samples [17].

However, in the case of the  $\beta$  relaxation the strict assignment to the only one type of molecular motion cannot be done. The multidimensional NMR investigations proved, that the  $\beta$  process consists of a  $180 \pm 10^\circ$  flip of the ester unit accompanied by restricted main chain rearrangements with an amplitude of about  $\pm 20^\circ$  [18,19]. Since complex features of the behaviour of the  $\beta$  process were proposed, also the dynamics of this relaxation demonstrates its complex nature.

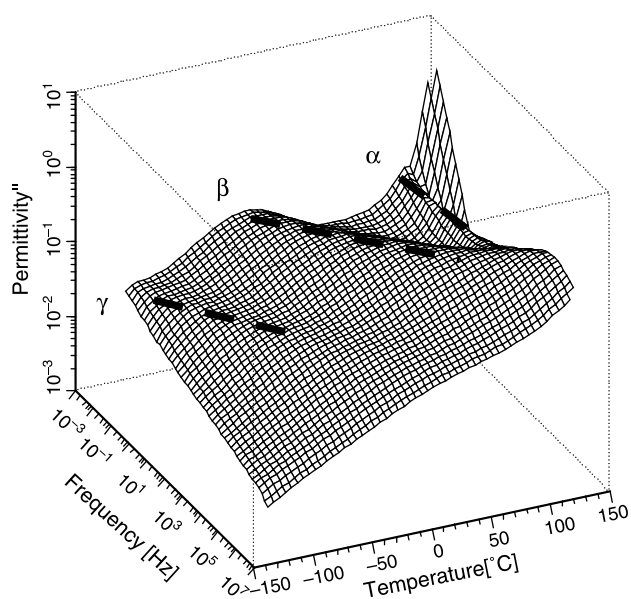


Fig. 2. 3-D map (frequency–temperature) dependences of  $\epsilon''$  for PMMA reference sample. The three dashed lines follow by visible relaxation processes -  $\alpha$ ,  $\beta$ ,  $\gamma$ .

The flipping of the side groups as well as their fluctuations around the equilibrium positions are equally possible and give contribution to the  $\beta$  relaxation [18,19].

The evolution of molecular mobility induced by aging in PMMA samples was investigated using the broadband dielectric spectroscopy mainly in a temperature range from  $-50$  to  $125$  °C. The representation of  $\text{tg } \delta (= \epsilon''/\epsilon')$  was chosen since it is not sensitive to changes of samples geometry during the experiments. Fig. 3 shows the comparison of the  $\tan \delta$  spectra at frequency of 1 Hz for the reference sample and samples aged at:  $95$  °C (Fig. 3(a)),  $80$  °C (Fig. 3(b)) and at room temperature during 9 months (Fig. 3(c)). The most pronounced changes in the dielectric spectra occur in the temperature range of around  $80$ – $90$  °C, in an intermediate region between the  $\alpha$  and  $\beta$  relaxations (the minimum), which is called Andrade zone [20]. This effect is not connected with the aging temperature because it appears not only for the samples aged at  $80$  and  $95$  °C (Fig. 3(a) and (b)) but also for the sample aged 9 months at  $25$  °C (Fig. 3(c)). Some correlation between the position of this minimum and the temperature and/or time of aging can be found. This minimum becomes deeper and it shifts towards higher temperature when aging is performed during longer time or at higher temperature (Fig. 3(d)). One can say that the overlapping of the  $\alpha$  and  $\beta$  relaxations decreases during the annealing and both relaxation processes become more separated. It is also visible that the aging leads to a narrowing of the  $\alpha$ -relaxation band. Such result suggests changes in the distribution of the relaxations times. For the samples aged at  $80$  and at  $95$  °C an increase of the amplitude of the  $\beta$ -relaxation can also be observed (Fig. 3(a) and (b)).

It is still not certain whether the  $\beta$ -relaxation in PMMA is affected by physical aging although it has been debated in the literature for long time [21–25]. In our studies the values of activation energy of this process were calculated for the samples after different thermal treatments. The calculations were made using the WinFit program (Novocontrol) in temperature range  $-15$  to  $20$  °C, in which the  $\beta$ -relaxation is clearly visible, well separated from other relaxations and conductivity contribution is negligible. The temperature dependence for this relaxation can be described by the Arrhenius equation. The obtained values of the activation energy for aged samples vary from  $76.8$  to  $79.4$  kJ/mol and are slightly higher comparing with the value for the reference sample ( $76.6$  kJ/mol). The observed increase is rather small, nevertheless, for all aged samples this tendency was found. In order to follow the evolution of the dielectric strength ( $\Delta\epsilon$ ) of the  $\beta$  relaxation during the physical aging the dielectric spectra were fitted using the Havriliak–Negami function (Eq. (4)) in the similar temperature range as mentioned before. The calculated values of  $\Delta\epsilon$  for the samples aged close to  $T_g$  are rather higher comparing with the reference sample. In the case of the sample aged at  $25$  °C during 9 months the calculated value of  $\Delta\epsilon$  is a little smaller comparing with the value for the reference sample. The parameters  $\alpha_{\text{HN}}$  and  $\beta_{\text{HN}}$  of  $\beta$ -relaxation were also determined. Their values calculated at  $10$  °C are presented in Table 1. The significant changes were observed in

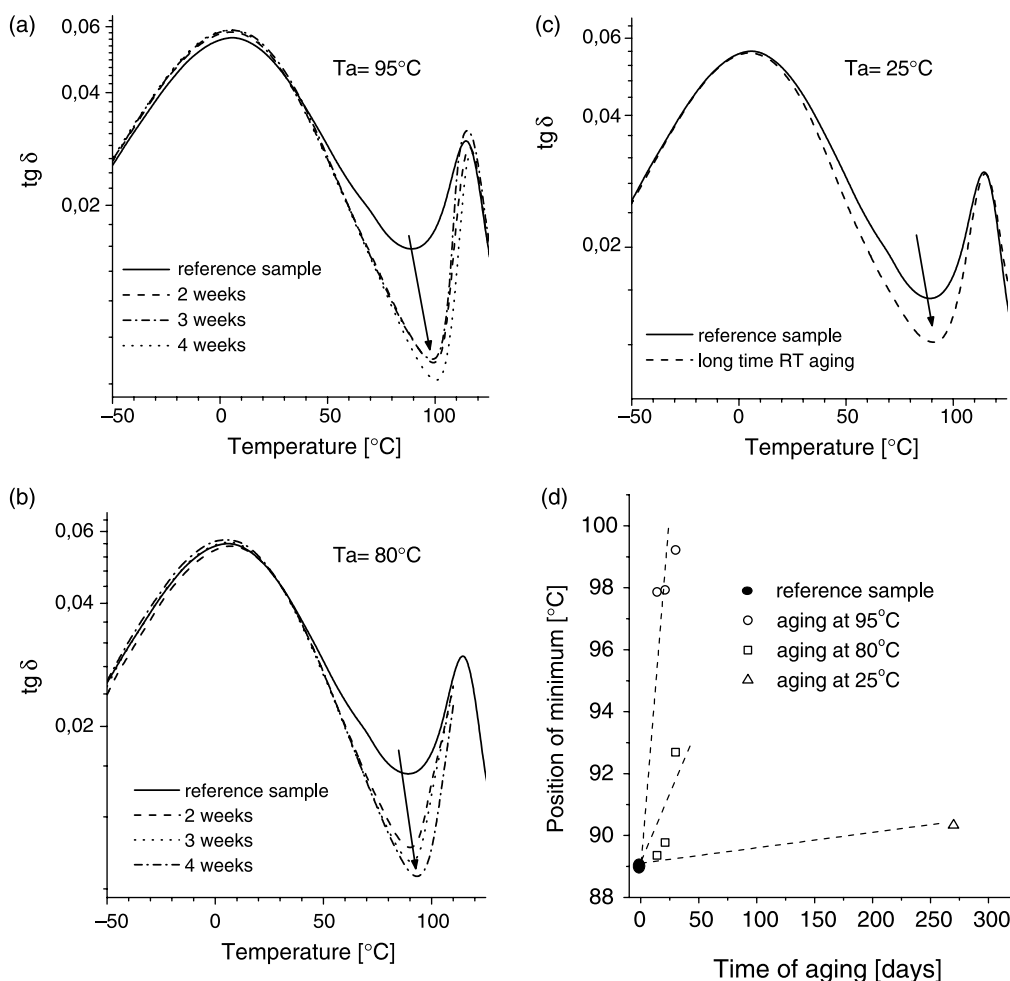


Fig. 3. The  $\text{tg } \delta$  spectra at frequency 1 Hz for the reference sample and samples aged at: 95 °C (a), 80 °C (b) and 25 °C during 9 months (c), respectively; (d) The positions of the so-called, ‘minimum’ between  $\alpha$  and  $\beta$  relaxation processes as a function of aging temperature and aging time. The lines on the graph are drawn as a guide for the eye.

the case of the  $\alpha_{\text{HN}}$  and the  $\beta_{\text{HN}}$  values calculated for the samples aged at 80 and 95 °C. The  $\alpha_{\text{HN}}$  decreases with aging, while the  $\beta_{\text{HN}}$  values change in the opposite direction. Such results correspond to the decrease of the width of the  $\beta$  relaxation, while its symmetry increases with aging.

Fig. 4 shows the LFHRMS measurements for the sample aged 3 weeks at 80 °C and for the quenched sample. It is visible that amplitude of the mechanical  $\beta$ -relaxation increases with aging. Similarly to the dielectric spectra one can observe better separation of the  $\alpha$  and  $\beta$ -relaxations after aging. Narrowing of the low temperature side of the  $\alpha$ -relaxation band after aging is again visible.

Table 1  
Havriliak–Negami fit parameters performed for  $\beta$  process at 10 °C for PMMA after different thermal treatments

	Temperature of aging (°C)	$\alpha_{\text{HN}}$	$\beta_{\text{HN}}$
Reference sample	–	0.396	0.501
Aged 9 months	25	0.394	0.507
Aged 3 weeks	80	0.391	0.516
Aged 3 weeks	95	0.387	0.540

In order to follow the changes of enthalpy during the physical aging the DSC measurements were performed. Fig. 5 shows thermograms for the PMMA samples recorded after different thermal histories. As a result of the aging, an

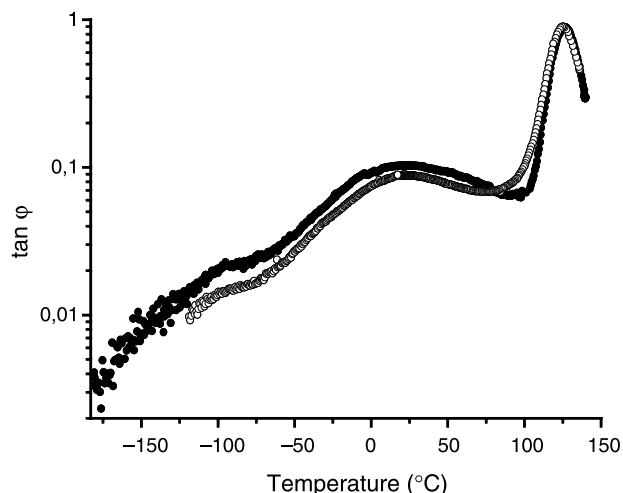


Fig. 4. Isochronal (frequency 1 Hz) mechanical  $\text{tg } \phi$  spectra for a sample aged 3 weeks at 80 °C (full circles) and the quenched sample (empty circles).

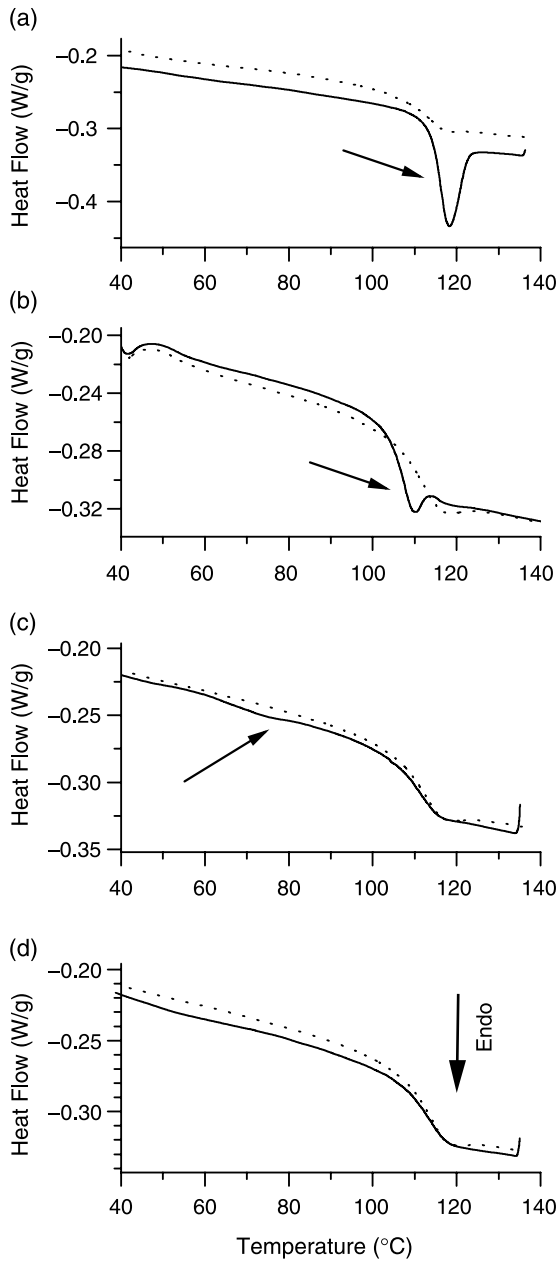


Fig. 5. The DSC thermograms for: (a) sample aged 3 weeks at 95 °C, (b) sample aged 3 weeks at 80 °C, (c) sample aged 9 months at 25 °C, (d) reference sample. The solid lines correspond to the first run and the dotted lines to the second run.

endothermic peak appears in the DSC thermograms during the first run (pointed by arrows) but it is absent in the second run (i.e. the annealing effect was erased during the first scan). This peak increases in magnitude and it appears at higher temperature when the aging is performed at temperature closer to  $T_g$ . Such effect of physical aging was reported earlier in literature [26,27] and was observed also for other thermally aged amorphous polymers like polystyrene [28] or poly(ethylene terephthalate) [29]. The calculations of the fictive temperature  $-T_f$  show that the  $T_f$  is the highest for reference sample (111 °C), while for the aged samples  $T_f$  values are smaller and equal: 103 °C (sample aged 3 weeks at

95 °C), 104 °C (sample aged 3 weeks at 80 °C) and 108 °C (sample aged 9 months at 25 °C).

#### 4. Discussion

The disordered amorphous network, as well as its heterogeneity at the nanoscale is well known and also sustained by computer simulations [30,31]. For our results to analyse the LFRS spectra we use a model of inhomogeneous nanoelasticity of amorphous polymers, whereby the Boson peak is interpreted as a VDOS excess corresponding to partially localised modes in cohesive nanodomains surrounded by softer zones, i.e. less cohesive channels [13]. This model connects LFRS spectra with a polymer network at the nanoscale, while the position of Boson peak -  $\omega_0$  (the lowest energy vibration mode which is localized in a cohesive domain) is related to the mean size of these domains (2a) by the following equation:

$$\omega_0 = S \frac{v}{2a} \quad (6)$$

where:  $v$  is the sound velocity in a domain and  $S$  is the shape factor. There is a size distribution of cohesive domains, which can be deduced from the width of Boson peak [13,32]. In the case of PMMA the average size of cohesive domains is found to be about 3 nm [32]. According to such model the intensity of the Boson peak (which is related to VDOS) decreases with a decreasing contrast between the cohesive nanodomains and the soft surrounding medium. Thus, the observed decrease of the Boson peak intensity with aging in Fig. 1 indicates that the nanostructure of atactic PMMA becomes more homogeneous with aging. Those results are in agreement with the previous inelastic neutron scattering measurements done for PMMA, which also exhibit the decrease of VDOS after thermal annealing [22]. In our results the decrease of intensity in Boson peak region after aging is observed for all aged samples, however, the changes are not identical in each case. This can be explained assuming a correlation between the frequency of the Boson spectral range and the activation energy of the relaxation, i.e. from Eq. (6), between the size of cohesive domains and the activation energy. Since the effect of aging is the more homogeneous cohesion or elasticity, it is deduced that the relaxations correspond to the hardening of the interfacial soft zones between cohesive domains. On the other hand, because the decrease of Raman intensity in the spectral range of the Boson peak extends to higher frequency when the temperature of aging increases, it comes that the activation energy of relaxation, i.e. of hardening, is the highest in soft zones between the smallest cohesive domains and vice-versa. In consequence, the relaxation in the process of aging takes place in the soft zones between the largest cohesive domains at room temperature, and it is spread in soft zones between cohesive domains from the large to small ones.

Small angle X-ray scattering (SAXS) was performed with the samples tested by LFRS. By extrapolation of the measured intensity to the transfer momentum  $Q=0$ , it is possible to estimate the amplitude of the density fluctuations, as it has recently been done [33,34]. Our measurements at room

temperature did not show any changes of the amplitude of density fluctuations after aging, even with the use of synchrotron sources. This is a confirmation that in case of PMMA the effect of aging decreases mainly the amplitude of cohesion or elasticity fluctuations and do not have any visible effect on the amplitude of electronic density fluctuations. However, it is not excluded that there exists a weak effect on the amplitude of density fluctuations, which are certainly concomitant with the cohesion fluctuations. As a matter of fact, a very weak change of density can induce a strong change of cohesion and molecular mobility.

Going from structural changes at nanometric level to molecular motions which allow this reorganization of the system it was observed by dielectric and mechanical measurements that aging affects mainly the intermediate region between  $\alpha$  and  $\beta$  relaxations. The primary relaxation is strongly affected at temperatures below  $T_g$  (glassy state) and due to this fact its width apparently decreases. These changes suggest that the annealing changes the broad distribution of relaxation times in case of the involved processes, while for the  $\alpha$  relaxation this effect seems to be the most visible. Furthermore, as one can conclude from dielectric measurements, the separation of the  $\alpha$  and  $\beta$  relaxations is more pronounced when aging is performed at higher temperature (Fig. 3). The value of  $\alpha_{HN}$  (Table 1) is the smallest for the sample aged during 3 weeks at 95 °C, while for the sample aged at 25 °C the  $\alpha_{HN}$  value is rather high and similar to reference state. Such changes reflect gradual narrowing of the  $\beta$  relaxation width during aging, while the increase in the  $\beta_{HN}$  parameter indicates an increase of the symmetry of this relaxation process.

The changes observed through dielectric and mechanical measurements can also be explained by the potential energy landscape. During aging the structure is subjected to structural relaxation by going above different energy barriers  $U(T)$ . The probability of the relaxation motions is proportional to  $\exp[-U(T)/kT]$ , so we can conclude that during aging at higher temperature the system allows to cross over smaller and higher energy barriers, while at low temperature only small energetic barriers are passed through. Going further, we can assume that the aging rate is faster at higher temperature. The system is going to reach equilibrium state in a shorter time (in our results the  $\alpha$  relaxation peak is apparently narrower for the sample aged at 95 °C than for the sample aged at 25 °C). This explanation is also appropriate for understanding the changes observed in our LFERS spectra. At this point it is interesting to make a correlation between the description of the dynamics of aging by the energy landscape and the model of inhomogeneous cohesion used to interpret the LFERS observations. The low energy barriers in the energy landscape correspond to the activation energies for the hardening of soft zones at the interface between larger cohesive domains while the higher ones correspond to the activation energies for the hardening of soft zones at the interface between smaller cohesive domains. The existence of the different relaxations which are responsible for the reorganization of the structure in the different size scales corresponds to broad and complex

distributions of the relaxation times which exist and become less dispersed by aging.

In a similar way we can explain changes of enthalpy during physical aging at different temperatures. The endothermic peak which appears on DSC thermogram is more pronounced and located closer to  $T_g$  when aging is performed at higher temperature (Fig. 5). The location of this peak close to  $T_g$  (the  $\alpha$  relaxation thermal zone) directly indicates that primary relaxation is involved in physical aging process. Nevertheless, even aging at 25 °C caused endothermic effect on DSC thermogram, which again confirms the broad range of dynamics in PMMA glass. The fictive temperature calculated from DSC thermograms correspond to an isostructural state of investigated glass and can be regarded as a parameter which reflects the departure of investigated state from equilibrium [2,29]. The reference sample is characterised by high fictive temperature reflecting its structural disorder. During aging the polymer reaches a state of lower energy characterised by lower fictive temperature. The aging is more efficient when performed at temperature closer to  $T_g$  (lower  $T_f$  values), while in case of aging at 25 °C the high  $T_f$  value reflects structural state distant from equilibrium.

In Fig. 3(a) and (b) it is visible that relaxation strength of the  $\beta$  process is higher for aged samples comparing with reference state. Such behaviour was also confirmed by calculations of the  $\Delta\epsilon$  performed for samples aged close to  $T_g$  using WinFit program. These results are contrary to the hypothesis of the existence of ‘islands of mobility’ as suggested by Johari to explain the behaviour of  $\beta$  relaxation [22]. It is believed that these ‘islands of mobility’ are like the loosely packed sites in the polymer structure where the molecules can orientate along different directions. As proposed by Johari the strength of  $\beta$  relaxation is decreasing during slow cooling or annealing. In the case of  $\beta$  relaxation and its involvement in structural changes caused by physical aging, there still is a debate [21–22,24–25]. In order to verify the observed difference in the behaviour of the  $\beta$  relaxation during aging, the in situ (isothermal) measurement was performed for about 43 h. Such protocol allows to avoid handling of the specimen between the two sets of results but can be applied for relatively short time of aging. During this measurement the temperature was 80 °C (i.e. 31 °C below  $T_g$ ) and its variation was <0.2 °C. The  $\epsilon'$ ,  $\epsilon''$  and  $\text{tg } \delta$  spectra in the frequency range  $2 \times 10^{-2}$  to  $10^6$  Hz were recorded every 20 min. A decrease of these dielectric observables after isothermal aging is clearly seen in Fig. 6(a)–(c), where plots of  $\epsilon'$ ,  $\epsilon''$  and  $\text{tg } \delta$  vs. frequency are shown for reference state and a sample aged 43 h at 80 °C, respectively. Indeed, the behaviour of the  $\beta$  relaxation proposed by Johari, i.e. the decrease of its amplitude with aging, occurs in the case of annealing during relatively short time at a temperature close to  $T_g$ , (Fig. 6), or during aging at temperature far from  $T_g$  (Fig. 3(c)). This can be explained taking into account the increase of the cohesion interactions in polymer at the beginning of aging. However, during further annealing an increase of the interaction in polymer makes its structure more homogeneous, as it was evidenced by LFERS experiments. The distribution of the relaxation times becomes

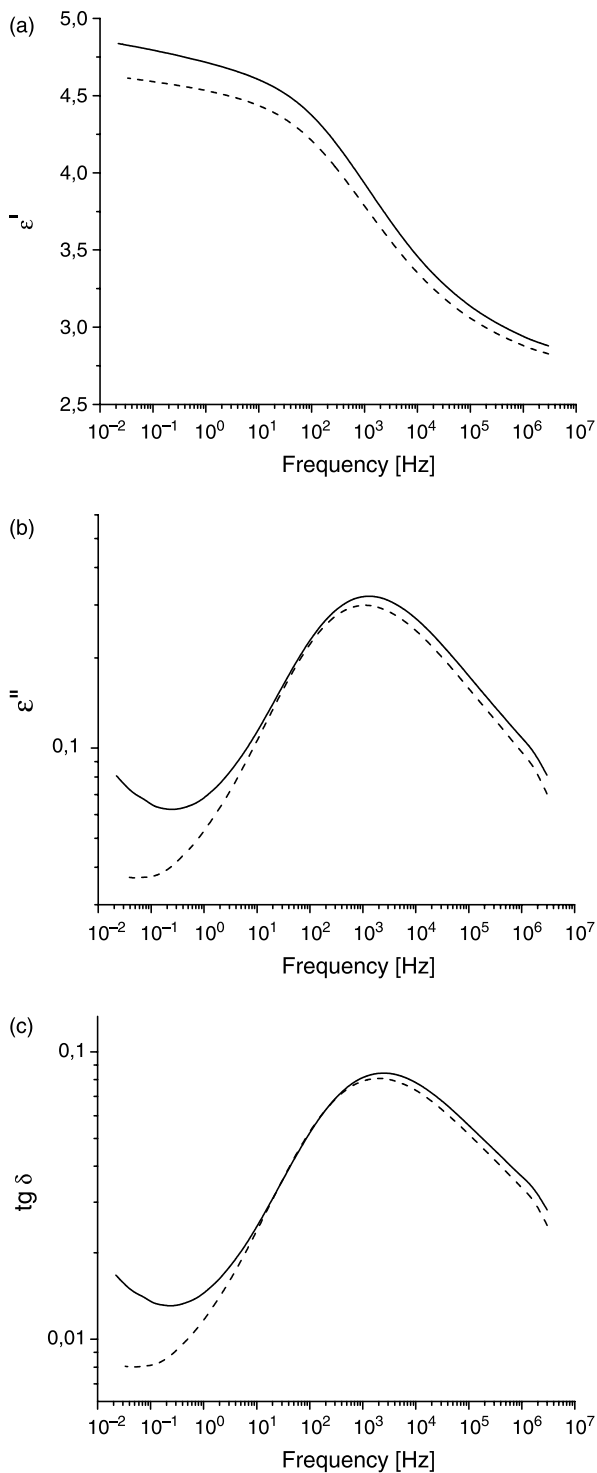


Fig. 6. The results of in situ aging performed at 80 °C. Representations of  $\epsilon'$ ,  $\epsilon''$  and  $\text{tg } \delta$  are shown vs. frequency in log scale, respectively (a), (b), (c). The solid line corresponds to reference sample (time of aging equal zero), while the dotted one was recorded for sample after 43 h of annealing.

less dispersed with aging and their amplitude can increase. In a Fig. 6 it can also be seen that the  $\beta$  relaxation apparently shifts to lower frequencies, i.e. to higher temperature in the temperature representation. Such changes confirm the increase of  $E_a$  for  $\beta$ -process after aging as it was calculated for samples aged in a longer time scale.

## 5. Conclusion

Low frequency Raman scattering, broadband dielectric and low frequency mechanical spectroscopy show that physical aging affects both nanostructure and molecular mobility of atactic PMMA. Aging makes the structure more homogenous by smoothing the elastic-constant contrast at the nanometric scale. The overlap of the  $\alpha$  and  $\beta$  relaxation diminishes during aging, which was clearly evidenced by dielectric and mechanical analysis. The mechanism of the physical aging process occurring at the molecular level is rather complex, however, an involvement of  $\alpha$  and  $\beta$  molecular relaxations in physical aging process is confirmed. The model of inhomogeneous cohesion or elasticity at the nanometric scale in glasses is able to interpret the decrease of Boson peak intensity as well as the changes of  $\alpha$  and  $\beta$  relaxations observed after aging, if the structural state of glass of lower energy corresponds to more homogenous cohesion at the nanometric scale.

## Acknowledgements

This work was partially supported by a French program: Mobilité Internationale Rhone Alpes (M.I.R.A.) and KBN project No. 4 T09A 147 25 (Poland) The authors thank Dr J.M. Lucas for performing SEC measurements.

## References

- [1] Struik LCE. Physical aging in amorphous polymers and other materials. Amsterdam: Elsevier; 1978.
- [2] Hodge IM. J Non-Cryst Solids 1994;169:211–66.
- [3] Gomez-Ribelles JL, Ribes-Greus A, Diaz-Calleja R. Polymer 1990;31:223–30.
- [4] Takahara K, Saito H, Inoue T. Polymer 1999;40:3729–33.
- [5] Perez J, Cavaille JY, David L. J Mol Struct 1999;479:183–94.
- [6] Davis WJ, Pethrick RA. Polymer 1998;39:255–66.
- [7] Schlosser E, Schönhals A. Polymer 1991;32:2135–40.
- [8] Diaz-Calleja R, Ribes-Greus A, Gomez-Ribelles JL. Polymer 1989;30:1433–8.
- [9] Etienne S, David L, Surovtsev N, Duval E. J Chem Phys 2001;114:4685–9.
- [10] Duval E, Saviot L, David L, Etienne S, Jal JF. Europhys Lett 2003;63(5):778–84.
- [11] Achibat T, Boukenter A, Duval E, Mermet A, Aboufaraj M, Etienne S, et al. Polymer 1995;36:251–7.
- [12] Etienne S, David L, Dianoux AJ, Saviot L, Duval E. J Non-Cryst Solids 2002;307–310:109–13.
- [13] Duval E, Boukenter A, Achibat T. J Phys Condens Matter 1990;2:10227–34.
- [14] Surovtsev NV, Mermet A, Duval E, Novikov VN. J Chem Phys 1996;104:6818–21.
- [15] Etienne S. Mat Sci Forum 1993;119–121:827–9.
- [16] Etienne S, Elkoun S, David L, Magalas LB. Mechanical spectroscopy and other relaxation spectroscopies. Solid State Phenom 2003;89:31–66.
- [17] McCrum NG, Read BE, Williams G. Anelastic and dielectric effects in polymer solids. New York: Wiley; 1967 [Chapter 8].
- [18] Schmidt-Rohr K, Kulik AS, Beckham HW, Ohlemacher A, Pawelzik U, Boeffel C, et al. Macromolecules 1994;27:4733–45.



- [19] Kuebler SC, Schaefer DJ, Boeffel C, Pawelzik U, Spiess HW. *Macromolecules* 1997;30:6597–609.
- [20] Donth E. *Relaxation and thermodynamics in polymer*. Berlin: Akademie Verlag GmbH; 1992.
- [21] Muzeau E, Perez J, Johari GP. *Macromolecules* 1991;24:4713–23.
- [22] Johari GP. *J Chem Phys* 1973;58:1766–70.
- [23] Muzeau E, Cavaille JY, Vassoille R, Perez J, Johari GP. *Macromolecules* 1992;25:5108–10.
- [24] Muzeau E, Johari GP. *Chem Phys* 1990;149:173–83.
- [25] Muzeau E, Vigier G, Vassoille R. *J Non-Cryst Solids* 1994;172–174: 575–9.
- [26] Andreozzi L, Faetti M, Giordano M, Palazzuoli D. *J Non-Cryst Solids* 2003;332:229–41.
- [27] Andreozzi L, Faetti M, Giordano M, Zulli F. *Macromolecules* 2005;38: 6056–67.
- [28] Hourston DJ, Song M, Hammiche A, Pollock HM, Reading M. *Polymer* 1996;37:243–7.
- [29] Abbès K, Vigier G, Cavaille JY, David L, Faivre A, Perez J. *J Non-Cryst Solids* 1998;235–237:286–92.
- [30] Yoshimoto K, Jain TS, Van Workum K, Nealey PF, de Pablo J. *J Phys Rev Lett* 2004;93:175501 [1–4].
- [31] Rossi B, Viliiani G, Duval E, Angelani L, Garber W. *Europhys Lett* 2005; 71:256–61.
- [32] Mermet A, Surovtsev NV, Duval E, Jal JF, Dupuy-Philon J, Dianoux AJ. *Europhys Lett* 1996;36(4):277–82.
- [33] David L, Vigier G, Etienne S, Faivre A, Soles CL, Yee AF. *J Non-Cryst Solids* 1998;235–237:383–7.
- [34] Levelut C, Faivre A, Le Parc R, Champagnon B, Hazemann JL, David L, et al. *J Non-Cryst Solids* 2002;307–310:426–35.